

Control of the defect in the liquid crystal director field on the slit of the patterned vertical alignment cell

Gi-Dong Lee,^{a),b)} Jung-Hee Son, and Yong-Hyun Choi
Department of Electronics Engineering, Dong-A University, Pusan 604-714, Korea

Jae-Jin Lju and Kyeong Hyeon Kim
AMLCD Division, Samsung Electronics Kiheung, Kyunggi-Do 449-711, Korea

Seung Hee Lee^{a),c)}
School of Advanced Materials Engineering, Chonbuk National University, Chonju-si, Chonbuk 561-756, Korea

(Received 13 September 2006; accepted 14 December 2006; published online 17 January 2007)

In this letter the authors studied the method to control the position of the generated defect on the slit of the patterned vertical alignment liquid crystal (LC) cell with dynamic stability. The authors modeled the LC director field with a defect on the slit and proposed an advanced wing pattern with a defect trap to stick the defect outside the active area. This shape can prevent the generation of the defect on the slit in the active area even if the authors increase the operation voltage, so that the LC dynamics on the slit is very stable and optical transmittance becomes higher. © 2007 American Institute of Physics. [DOI: 10.1063/1.2432251]

The demand for large-area flat panel display televisions (TVs) has been increased by the expansion of the digital TV market. Liquid crystal displays (LCDs) occupy a prominent position in the flat panel display market, and these days the LCD market size is rapidly growing. LCD TVs have the advantages of high resolution, light weight, slim thickness, etc. In order to maximize electro-optical characteristics, many companies and research groups have been developing advanced technology for LCD display quality. In particular, patterned vertical alignment (PVA) technology,¹ developed by Samsung Electronics as a practical and wide-viewing angle mode, is one of the most useful modes for large-sized application. PVA characteristics include a multidomain structure formed by a fringe-field effect and optical compensation by retardation films.^{2,3} In general, however, liquid crystal (LC) cells using the multidomain effect for wide viewing show relatively low transmittance because the nonuniform voltage distribution due to patterned electrodes can make the active area of the PVA cell have strong energy locally, so that defects can occur in the active area.

The generated defect can affect both the dynamic stability and the optical transmittance. LC dynamics near the edge of the slit is very unstable because there is a strong competition for the LC director's strain energy around the active area and edge on the wing pattern, so that we can easily find an unstable defect line on the slit. A conventional PVA mode uses a notch structure around the center of the slit to prevent the generated defect from moving when we apply the voltage, as shown in Fig. 1. However, this structure can also make another defect between the notch structure around the center of the slit and the edge of the slit. In addition, a defect that is generated by the notch structure on the slit and the edge of the slit moves to the active area when the voltage is increased. In this letter, we simulate and model the LC director field with a defect on the slit with a notch pattern. In

order to remove the induced defect on the slit of the active area by the notch pattern and the slit edge, we propose an advanced shape of the slit edge (wing pattern) with excellent dynamic stability, which can prevent the defect from moving to the active area. We compare the electro-optical characteristics of the LC director by the proposed electrode structure cell with the conventional electrode structure by using three-dimensional simulation.

In general, the conventional PVA cell without the notch structure in the center of the slit demonstrates very unstable dynamic behavior because the generated defect due to the competition of the strain energy from the slit edge moves along the slit by the application of voltage. The dynamic instability of the LC director field is shown in Fig. 2. The dotted ellipse points represent the slit with the notch structure, and the solid ellipse represents the slit without the notch structure. In the figure, we can find different dynamic responses of the LC director to the applied voltage between the

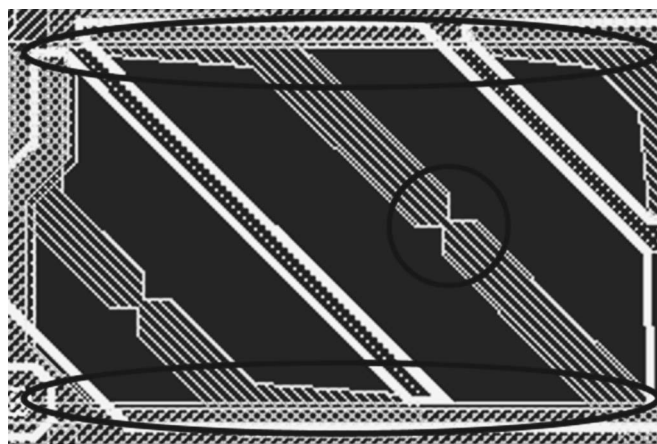


FIG. 1. Structure of the PVA cell. The diagonal lines in the active area represent the slits, which consist of two slits with a notch pattern on the upper substrate (striped line) and two slits on the lower substrate. The solid circle represents the notch pattern in the center of the slit. The elliptical circle represents the edge with wing pattern.

^{a)} Authors to whom correspondence should be addressed.

^{b)} Electronic mail: gdllee@dau.ac.kr

^{c)} Electronic mail: lsh1@chonbuk.ac.kr

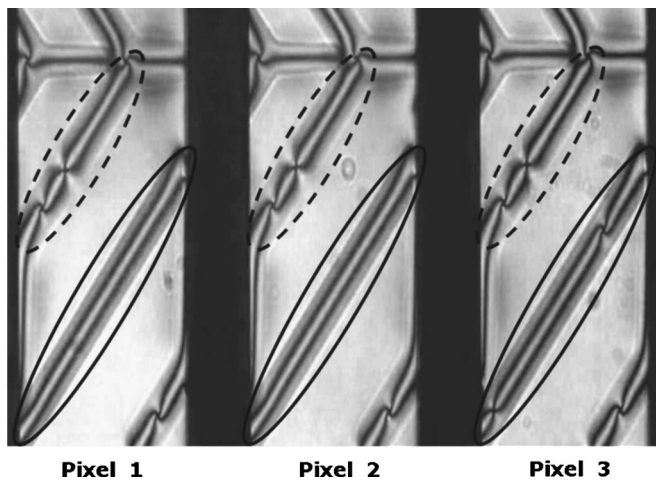


FIG. 2. Microscopic photograph of the PVA cell in the bright state.

experimental pixels. The slit of the PVA cell with the notch structure shows the same dynamic behaviors between pixels. On the contrary, without the notch structure, we can observe that the defect is generated in pixel 3, and not generated in pixels 1 and 2 even if we apply the same voltage to the cell. The generated defect on the slit without the notch pattern moves along the slit by the application of voltage and shows very unstable electro-optical characteristics. Therefore, the notch structure applied to the electrode structure can lead to very stable dynamic behavior of the defect. On the contrary, however, the notch structure in the center of the slit can generate another defect. In Fig. 2, we can find two positions of the defect on the slit with the notch pattern (the dotted ellipse region). A defect on the upper position is caused by the notch, and we can observe another defect on the lower position, which is induced by the nonuniform voltage distribution around the edge of the slit and the notch structure. Therefore, the notch structure in the middle of the slit can prevent the dynamic instability of the LC director field, but can induce another defect on the slit of the PVA cell.

In order to achieve the LC configurations in the equilibrium state, we need to calculate the minimum free energy. For the calculation of the free energy, we use Gibb's free energy of the LC cell that is composed of elastic constants and electric field terms. In general, the elastic energy can be expressed with the Oseen-Frank vector representation that uses three elastic constants (splay, twist, and bend) and Q -tensor representation method.⁴⁻⁸ However, the Oseen-Frank equation with the vector form cannot exactly describe the director orientation in the local area that stores high elastic deformation energy because the equation depends on the sign of the unit vector describing the director field. On the contrary, recent studies have provided that the numerical modeling method with the Q -tensor form can exhibit more exact results in the local area with high deformation energy, which may induce the defect and the phase transitions between topologically different states.⁶⁻⁸ As for the PVA cell, it also contains local points on the slit with very high elastic deformation energy, obtained by applying the voltage, so that the Q -tensor method is more suitable for modeling the LC director configuration in the PVA cell.

In order to compare the modeling to the experimental result, we set geometric parameters to the same values as the real panel, as shown in Fig. 1. The distance between the slits

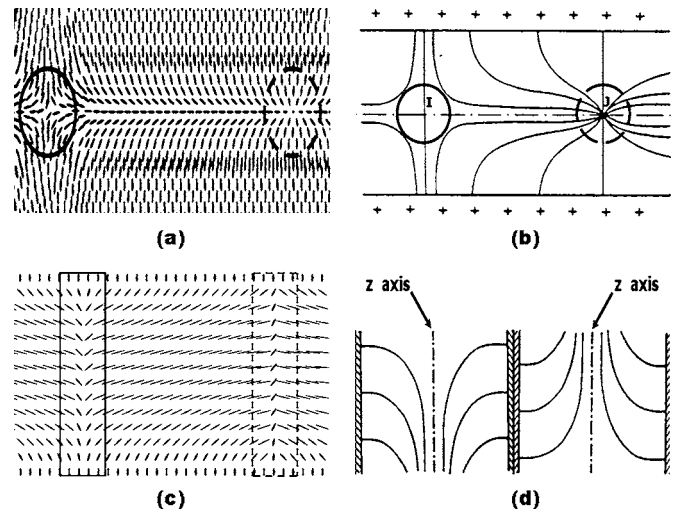


FIG. 3. Modeling of the LC director field of the PVA cell with notch pattern: (a) modeled LC director field in the top view, (b) a cartoon of the director orientation with defect for the top view, (c) modeled LC director field in the cross-sectional view, and (d) a cartoon for modeled LC director field with defect.

is $20 \mu\text{m}$, the width of the slit is $10 \mu\text{m}$, and the cell gap was set to $3.8 \mu\text{m}$. The parameters of the used LC are as follows: $k_{11}=12.7$, $k_{22}=6$, $k_{33}=15.3$, $\gamma=0.133$, $\epsilon_{\parallel}=3.6$, and $\epsilon_{\perp}=7.4$.

Figure 3(a) shows three-dimensional modeling of the LC director field on the slit with the notch structure in the middle layer of the LC director. The director configuration in the solid circle represents the defect generated by the notch structure in the center of the slit, and that in the dotted circle represents the defect due to the competition of the strain energy by the edge of the slit and the notch structure of the center. The defect by the notch pattern [the solid circle in Fig. 3(a)] shows a point disclination which has a Frank index $n=-2$ with strength $s=-1$. In general, point disclination with $s=1$ can be performed in two ways, upward and downward directions.⁹ The upward portion and the downward portion are linked, which are centered by two singular points. Therefore, the notch pattern on the slit can induce another point disclination with a Frank index $n=2$ with strength $s=1$. The dotted circle in Fig. 3(a) shows the induced disclination line by the defect from the notch pattern. The position of the induced defect on the slit can be decided by the boundary condition of the slit edge. Figure 3(b) shows the cartoon of the modeling of the singular point for Fig. 3(a) with Frank index $n=\pm 2$ and strength $s=\pm 1$.⁹ Figures 3(c) and 3(d) show the cross-sectional view of the simulated LC director field with the induced defect and cartoons for modeled LC director field with the defect, respectively. In the figure, we can observe the "escape" of the disclination to the downward direction, so that the distortion around a centerline with $s=-1$ is continuously transformed into a smooth deformation with no singular line. On the contrary, the induced disclination on the slit also escaped to the upward direction and shows the continuous LC director profile. The cartoon in Fig. 3(d) describes the escape of the point disclinations with $s=\pm 1$.⁹ The difference between Figs. 3(c) and 3(d) can be observed near the surface of the substrate because the cartoon in Fig. 3(d) applies infinite boundary along the z direction.

The notch pattern of the slit plays a very important role to prevent instability of the LC director field with the defect.

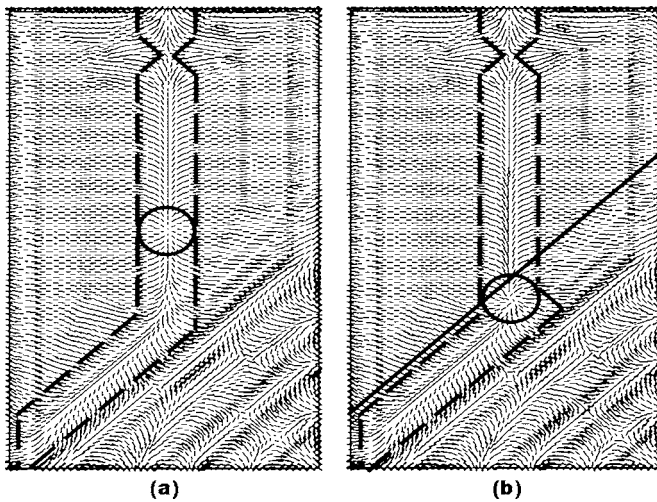


FIG. 4. Comparison of LC director field with defect: (a) the LC director distribution by the conventional slit and (b) the LC director distribution by the advanced slit with defect trap. The dashed line represents the slit pattern, and the solid line represents the boundary of the active area and the black matrix. The upper area of the solid line will be the active area and the lower area of the solid line will be the black matrix area.

As previously noted, however, the notch pattern of the slit intrinsically follows another defect with opposite strength. In this letter, therefore, we propose the defect trap at the edge of the slit, which can stick the induced defect outside the active area. Figure 4 shows the comparison of the LC director field with the defect by the conventional slit and the advanced slit with the defect trap. In order to take the defect by the notch structure out of the active area, we applied the advanced shape of the slit, as shown in Fig. 4(b). In order to push the defect to the edge of the slit, we need to make a geometric position, which can store strong elastic energy on the edge, as shown in Fig. 4(b). The solid circle indicates the defect trap structure in the slit edge to fix the induced defect. The defect trap in the slit edge moves the induced defect ($s=+1$) to the position of the defect trap on the slit edge, which is outside the active area, so that the induced defect by the slit edge and the notch structure in the center are always out of the active area even if we change the applied voltage. In Fig. 4(b), we observe that the defect trap structure on the edge of the slit effectively prevents the induced defect from moving to the active area compared to the conventional cell in Fig. 4(a). Figure 5 shows the comparison of the calculated optical transmittance of the PVA cell with the defect trap and without the defect trap on the slit edge. A black area represents the black mask. We can observe that the optical loss by the induced defect can be effectively removed because the position of the induced defect moves under the black matrix area. The calculated response time of the proposed structure was 3.7 ms, which is almost the same as that of the conventional structure. However, optical transmittance of the proposed structure was higher (2.3 a.u.) compared to the

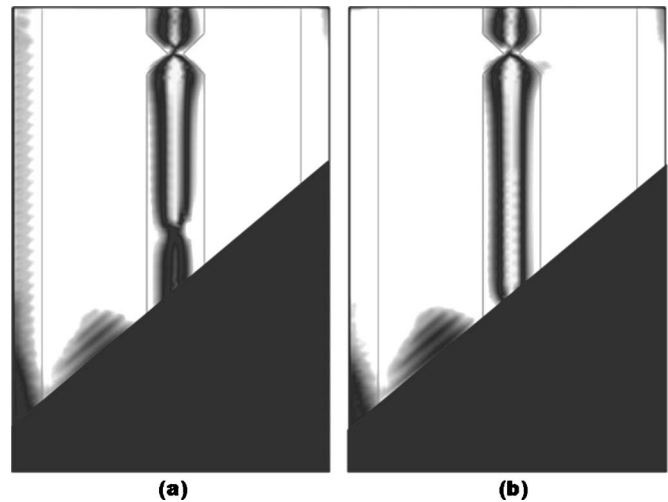


FIG. 5. Comparison of the calculated optical transmittance: (a) optical transmittance by the conventional slit and (b) optical transmittance by the advanced slit with defect trap.

conventional structure (19.7 a.u.) on the slit area. Calculation has been done using the commercial software TECHWIZ LCD (Sannayi-system, Korea), which applies the Q -tensor method to calculate the LC director field.

In conclusion, we simulated the LC director field with the defect in the PVA LC cell with the notch structure on the slit. We observed a pair of defects on the slit and modeled the defect by the Q -tensor method ($s=\pm 1$). We proposed the defect trap on the slit edge, which can effectively push the induced defect outside the active area. In order to verify the effect of the defect trap on the slit, we modeled the motion of the defect on the slit and confirmed that the defect is trapped on the edge of the slit, which is outside the active area, even though we increased the voltage.

This work was supported in part by Samsung Electronics and partly by the Ministry of Information and Communication (MIC), Korea, under the Information Technology Research Center (ITRC) support program supervised by the Institute of Information Technology Advancement (IITA) (IITA-2006-C109006030030).

¹S. S. Kim, SID Int. Symp. Digest Tech. Papers **35**, 760 (2004).

²K. H. Kim, K. H. Lee, S. B. Park, J. K. Song, S. N. Kim, and J. H. Souk, IDRC Asia Display '98, 21-4 (1998), p. 383.

³K. H. Kim, J. J. Ryu, S. B. Park, J. K. Song, B. W. Lee, J. S. Byun, and J. H. Souk, IMID '01 Digest (2001), p. 58.

⁴K. Schiele and S. Trimper, Phys. Status Solidi B **118**, 267 (1983).

⁵D. W. Berreman and S. Meiboom, Phys. Rev. A **30**, 1955 (1984).

⁶S. Dickmann, J. Eschler, O. Cossalter, and D. A. Mlynski, SID Int. Symp. Digest Tech. Papers **24**, 638 (1993).

⁷G. D. Lee, J. Anderson, and P. J. Bos, Appl. Phys. Lett. **81**, 3951 (2002).

⁸G. D. Lee, P. J. Bos, S. H. Ahn, and K. H. Kim, Phys. Rev. E **67**, 041715 (2003).

⁹P. G. de Gennes and J. Prost, *The Physics of Liquid Crystals*, 2nd ed. (Clarendon, Oxford, 1993), 181, 186.